

## The Role of Glucuronidation and P450 Oxidation in the Bioactivation of Bromfenac

James P. Driscoll, Aprajita S. Yadav, and Nina R. Shah

*Chem. Res. Toxicol.*, **Just Accepted Manuscript** • DOI: 10.1021/acs.chemrestox.7b00293 • Publication Date (Web): 23 Mar 2018

Downloaded from <http://pubs.acs.org> on March 29, 2018

### Just Accepted

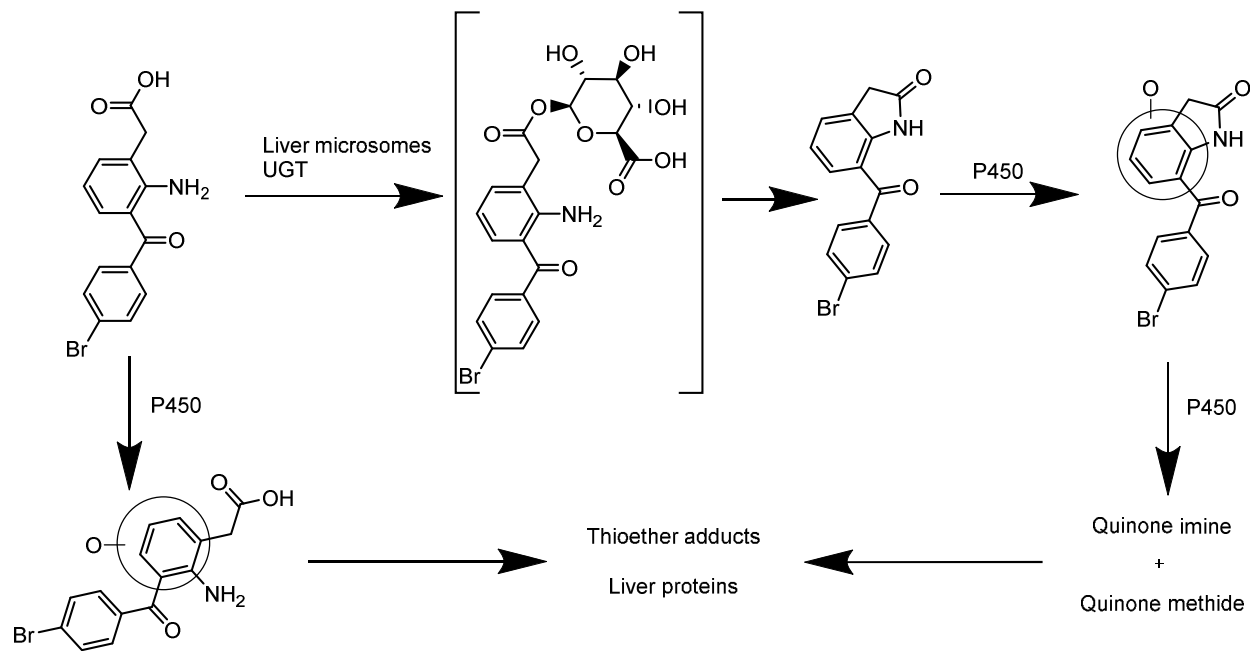
“Just Accepted” manuscripts have been peer-reviewed and accepted for publication. They are posted online prior to technical editing, formatting for publication and author proofing. The American Chemical Society provides “Just Accepted” as a service to the research community to expedite the dissemination of scientific material as soon as possible after acceptance. “Just Accepted” manuscripts appear in full in PDF format accompanied by an HTML abstract. “Just Accepted” manuscripts have been fully peer reviewed, but should not be considered the official version of record. They are citable by the Digital Object Identifier (DOI®). “Just Accepted” is an optional service offered to authors. Therefore, the “Just Accepted” Web site may not include all articles that will be published in the journal. After a manuscript is technically edited and formatted, it will be removed from the “Just Accepted” Web site and published as an ASAP article. Note that technical editing may introduce minor changes to the manuscript text and/or graphics which could affect content, and all legal disclaimers and ethical guidelines that apply to the journal pertain. ACS cannot be held responsible for errors or consequences arising from the use of information contained in these “Just Accepted” manuscripts.

1  
2  
3  
4  
5  
6  
7 The Role of Glucuronidation and P450 Oxidation in  
8  
9  
10  
11 the Bioactivation of Bromfenac  
12  
13  
14  
15

16 *James P. Driscoll\*, Aprajita S. Yadav and Nina R. Shah*  
17

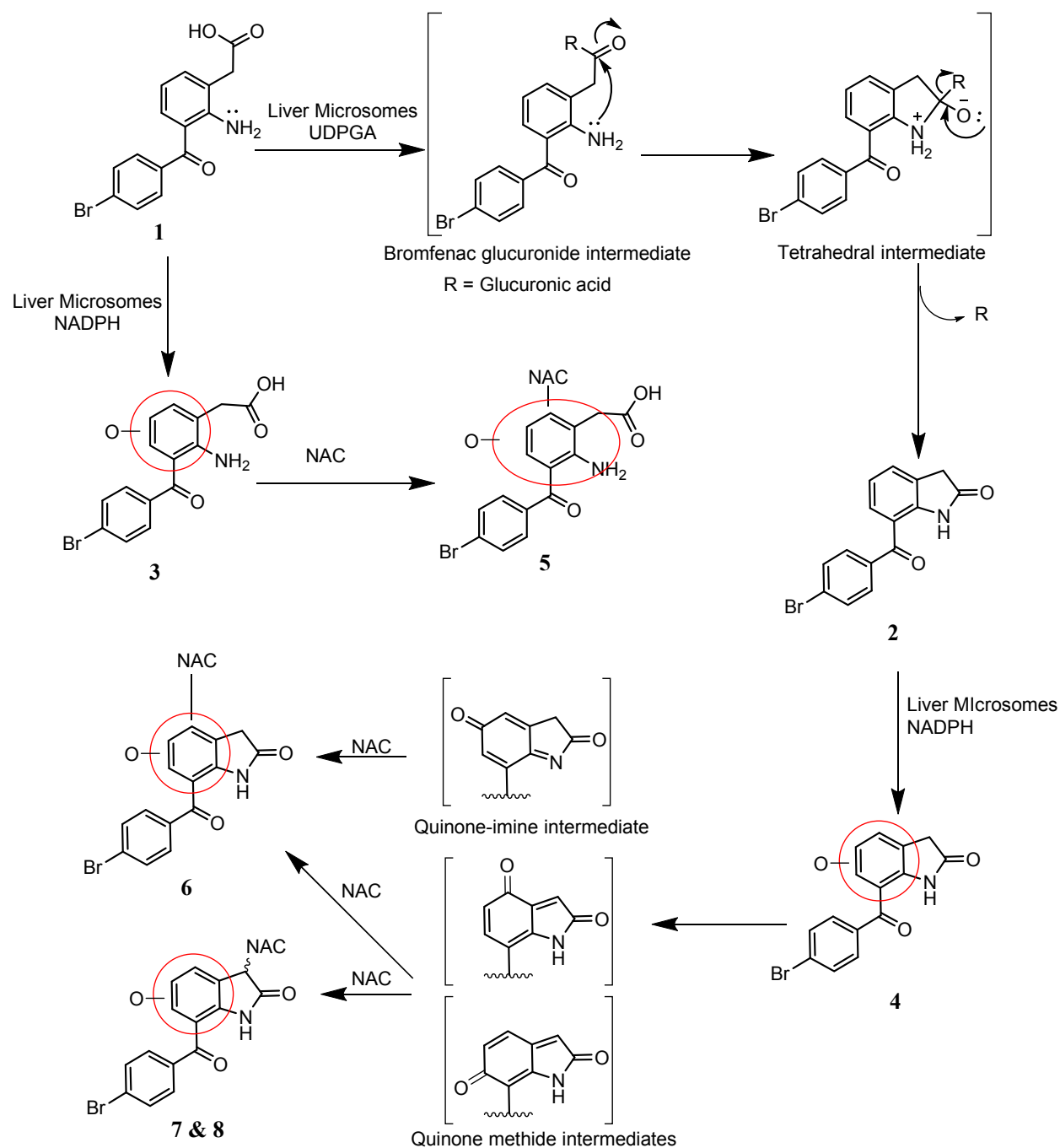
18  
19 MyoKardia Inc, 333 Allerton Ave. South San Francisco, CA 94080  
20  
21  
22  
23  
24  
25  
26  
27  
28  
29  
30  
31  
32  
33  
34  
35  
36  
37  
38  
39  
40  
41  
42  
43  
44  
45  
46  
47  
48  
49  
50  
51  
52  
53  
54  
55  
56  
57  
58  
59  
60

TOC graphic



1  
2  
3 **ABSTRACT** Bromfenac is a nonsteroidal anti-inflammatory drug which was approved in the  
4 United States in 1997. It was withdrawn from clinical use less than one year later, in 1998, due  
5 to hepatotoxicity. We investigate the potential of bromfenac to be metabolized to reactive  
6 intermediates to further the current understanding of bromfenac bioactivation. Incubations were  
7 conducted with hepatocytes and human, rat and cynomolgus liver microsomes fortified with  
8 cofactors and N-acetylcysteine. One thioether adduct of hydroxylated bromfenac and three  
9 thioether adducts of hydroxylated bromfenac indolinone were detected in extracts following  
10 incubations in liver microsomes fortified with NADPH and UDPGA. These findings  
11 demonstrate a bioactivation pathway for bromfenac and contribute to the body of evidence which  
12 could advance the understanding of the toxicity associated with bromfenac.  
13  
14  
15  
16  
17  
18  
19  
20  
21  
22  
23  
24  
25  
26  
27  
28  
29  
30  
31  
32  
33

34 **Introduction** Bromfenac (Duract) is a nonsteroidal anti-inflammatory drug (NSAID) used for  
35 the treatment of osteoarthritis, rheumatoid arthritis, ankylosing spondylitis, and acute muscle  
36 pain. Bromfenac (**1**) was approved in the United States in 1997 for a duration of use of less than  
37 10 days. The drug was voluntarily withdrawn in 1998 due to adverse reactions to **1** including  
38 hepatic necrosis, cholestasis and fatal liver failure.<sup>1,2</sup> In many cases of bromfenac associated  
39 hepatotoxicity there was a significant increase in liver alanine aminotransferase (ALT), aspartate  
40 aminotransferase (AST) and alkaline phosphatase (AP) levels. Patients taking the drug for more  
41 than 10 days had a higher risk of developing liver injury or failure.<sup>3</sup>  
42  
43  
44  
45  
46  
47  
48  
49  
50  
51  
52  
53  
54  
55  
56  
57  
58  
59  
60



**Scheme 1. Proposed bioactivation pathway for bromfenac. NAC = *N*-acetylcysteine**

In mass balance studies, healthy volunteers were dosed with  $^{14}\text{C}$ -labeled **1** and bromfenac indolinone (**2**) (Scheme 1) was found to be the major metabolite in urine. No evidence was found for the formation of thioether-linked metabolites.<sup>4</sup> In preclinical toxicology studies with rats, **1**

1  
2  
3 was found to cause vacuolar changes, necrosis and cytological alterations to hepatocytes, and  
4 glutathione depletion in the liver and kidney. The compound was also found to cause papillary  
5 necrosis of the kidney and caused cytological alterations of hepatocytes in mouse carcinogenicity  
6 studies.<sup>5</sup> *In vitro* evidence suggests that in the presence of NADPH and UDPGA, the amount of  
7 covalent binding of **1** to human liver microsomal protein is increased when compared with  
8 NADPH alone.<sup>6</sup> The *in vitro* covalent binding result suggests that bioactivation could proceed  
9 through a glucuronidation pathway, although an acyl glucuronide metabolite was never detected  
10 in human radiolabeled studies and could not be synthesized.<sup>7,4</sup>  
11  
12  
13  
14  
15  
16  
17  
18  
19  
20  
21

22 Chemical structural motifs in drug-like molecules that are known to cause drug induced liver  
23 injury (DILI) are known as structural alerts or toxicophores.<sup>8</sup> Bromfenac contains three different  
24 known structural alerts; an aniline, a bromobenzene ring, and a phenylacetic acid.<sup>9,10,11</sup> Many of  
25 the adverse events associated with bromfenac affect the liver, therefore it is possible that  
26 formation of reactive metabolites are involved in observed adverse events. However, such  
27 reactive metabolites have not yet been reported to the authors' knowledge.  
28  
29  
30  
31  
32  
33  
34  
35  
36

37 The purpose of this work is to investigate the metabolism of **1** to determine if these  
38 toxicophores play a role in the formation of reactive metabolites. Incubations were performed  
39 with **1** in human hepatocytes and human, rat and monkey liver microsomes supplemented with  
40 UDPGA, NADPH and thiols, such as glutathione and *N*-acetylcysteine. During our  
41 investigations, we found evidence for the formation of novel thioether adducts of hydroxylated  
42 bromfenac (**3**) and the hydroxylated indolinone metabolite (**4**). We also found that the formation  
43 of **2** is likely catalyzed by uridine 5'-diphospho-glucuronosyltransferase (UGT).  
44  
45  
46  
47  
48  
49  
50  
51  
52  
53  
54  
55  
56  
57  
58  
59  
60

## Materials and Methods

**Materials.** N-acetylcysteine (cat number A7250-50G), Bromfenac Sodium (cat number SML0289-50MG), Carbamazepine (cat number 94496-100MG), Glutathione (cat number G6529-25G), L-Glutamine (cat number G6392-1VL), and Williams' Medium E (cat number W1878-500ml) were purchased from Sigma (St Louis, MO). All solvents used for LC/MS analysis were of chromatographic grade and purchased from Fisher Scientific. Stock solutions of bromfenac and bromfenac indolinone were prepared as solutions in dimethyl sulfoxide (20 mM). Human hepatocytes (20 donor pool), human (pooled), rat and cynomolgus monkey liver microsomes were purchased from BioreclamationIVT (Baltimore, MA). Potassium Phosphate buffer (Cat No J62397) was purchased from Alfa Aesar (Ward Hill, MA)

**Bromfenac Indolinone Synthesis.** The bromfenac indolinone standard was synthesized from bromfenac sodium obtained from Sigma. 21 mg of bromfenac was dissolved in 5 ml of water. 2 ml of 6N hydrochloric acid was added and a white precipitate immediately formed. The resulting saturated solution was vacuum filtered and the filtrate was dried under vacuum for 24 hours. A 1 mg sample was dissolved in DMSO-d<sub>6</sub> (D, 99.8%, Cambridge Isotope) containing 0.05% V/V TMS as an internal chemical-shift reference standard, and transferred to a 3 mm NMR tube, purged with nitrogen, and sealed. The <sup>1</sup>H NMR of the synthesized material is consistent with the structure of the indolinone (Figure 1).

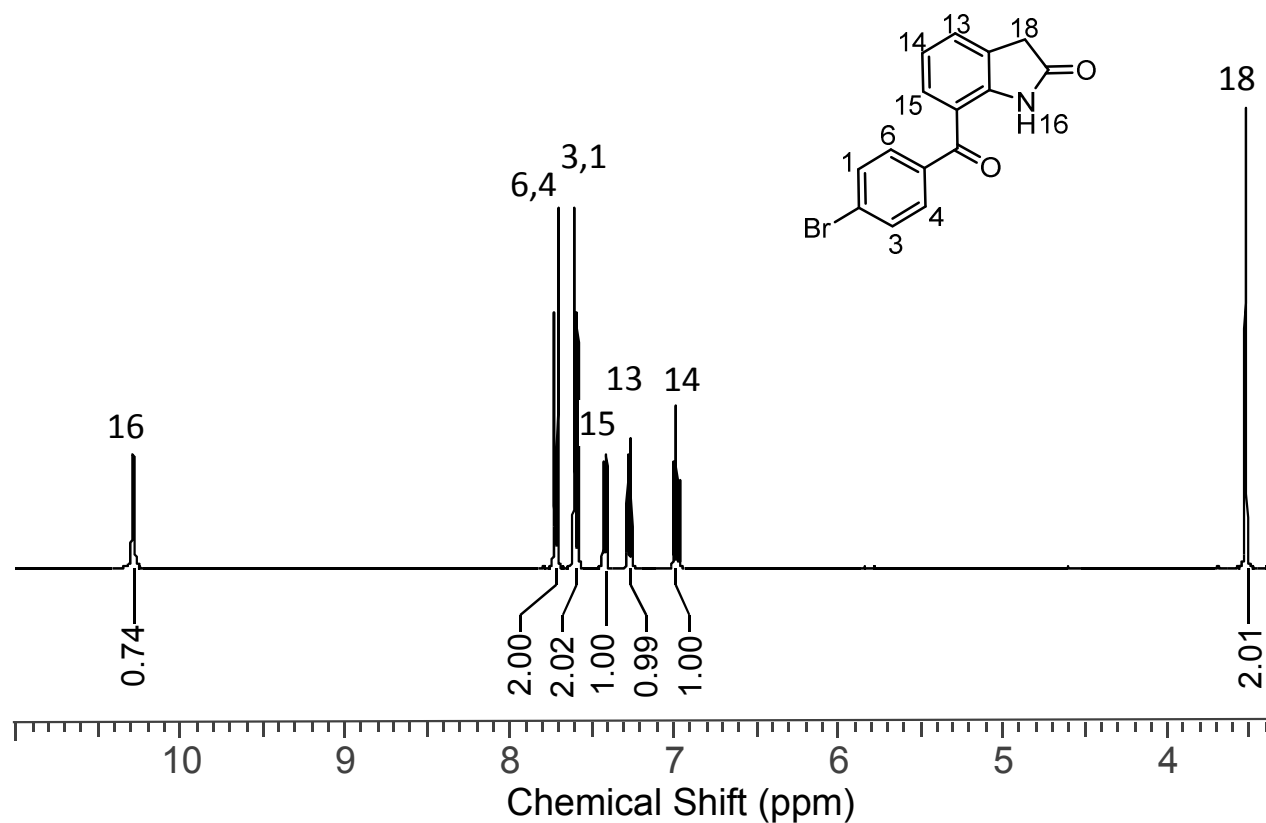


**Figure 1.**  $^1\text{H}$  NMR of **2**. Collected on a Bruker Ascend<sup>TM</sup> (400 MHz in DMSO- $d_6$ )  $\delta$ : 10.29 (s, 1H), 7.72 (d,  $J=8.44$  Hz, 2H), 7.56-7.64 (m, 2H), 7.93-7.45 (m, 1H), 7.24-7.30 (m, 1H), 6.94-7.02 (m, 1H), 3.52 (s, 2H).

**Metabolite Identification Studies.** Metabolite identification experiments were performed to determine the fate of **1** (20  $\mu\text{M}$ ) and **2** (20  $\mu\text{M}$ ) in human, rat and cynomolgus monkey liver microsomes (1 mg protein/ml). Incubations were conducted in potassium phosphate buffer (0.1 M, pH 7.4) in either the presence or absence of NADPH (1 mM) and UDPGA (1 mM). All incubations included NAC (5 mM), alamethicin (10  $\mu\text{g/ml}$ ), and  $\text{MgCl}_2$  (5 mM). 10 ml total volume reactions were performed in 20 ml glass scintillation vials in a shaking water bath (low speed, 37°C). A metabolite identification study was performed as above with  $\beta$ -mercaptoethanol

1  
2  
3 (0.1 mM) as the nucleophilic thiol. Since  $\beta$ -mercaptoethanol has been shown to inhibit  
4  
5 cytochrome P450 at higher concentrations, the concentration was chosen to be three times lower  
6  
7 than the lowest  $IC_{50}$ .<sup>12</sup>  
8  
9

10 Incubations with glutathione were performed with **1** (20  $\mu$ M) in human hepatocytes (1 million  
11  
12 cells/ml) and human liver microsomes (1 mg protein/ml). Microsome incubations were  
13  
14 conducted in potassium phosphate buffer (0.1 M, pH 7.4) in the presence of NADPH (1 mM),  
15  
16 UDPGA (1 mM) and glutathione (5 mM). Hepatocyte incubations included glutathione (5 mM)  
17  
18 in William's E media which was added to the cells to bring the concentration to 1 million  
19  
20 cells/ml. Microsome incubations were performed at 8 ml volume reactions and hepatocyte  
21  
22 incubations were performed at 5 ml total volume in 20 ml glass scintillation vials in a shaking  
23  
24 water bath (low speed, 37°C).  
25  
26  
27

28 All reactions were quenched after one hour with an equal volume of acetonitrile (ACN),  
29  
30 capped, and vortex-mixed (1 min) then were centrifuged (14,000 rpm, 5 min). Supernatants were  
31  
32 transferred to glass 13  $\times$  100 mm tubes and evaporated in a Speed Vac® Plus SC210A Savant  
33  
34 system (Savant Instruments, Inc. Farmingdale, NY) under vacuum. Once dried, extracts were  
35  
36 reconstituted with a solution containing ACN and water (1 mL, 1/1, v/v). The reconstituted  
37  
38 mixtures then were transferred to microcentrifuge tubes and centrifuged (14,000 rpm, 5 min).  
39  
40 The resulting supernatants were transferred to high-performance liquid chromatography vials.  
41  
42  
43

#### 44 **LC-MS/MS Conditions for Metabolite Identification Studies.**

45  
46  
47 High resolution LC-MS/MS analyses was conducted using a Dionex Ultimat 3000 HPLC  
48  
49 (Thermo Fisher Scientific, Waltham, MA) equipped with a binary pump, degasser, ultraviolet  
50  
51 detector, CTC autosampler, and column heater kept at 25°C. The injection volume was 50  $\mu$ l.  
52  
53  
54 Chromatographic resolution was achieved with a ThermoScientific (Waltham, MA) BetaBasic  
55  
56  
57  
58  
59  
60

1  
2  
3 C18 column (4.6 × 250 mm, 3µm). Mobile phases consisted of 0.1% aqueous formic acid  
4 (solvent A) and acetonitrile with 0.1% formic acid (solvent B) run at a constant flow rate of 0.7  
5 ml/min. The solvent gradient was initially held at 0% solvent B for 0.1 min and increased  
6 linearly to 100% solvent B over 53 min, kept at 95% solvent B for an additional one min, then  
7 immediately dropped to 5% solvent B over 0.5 min, where it was held constant at 0% solvent B  
8 for 5.5 min before the next sample injection (20 µl). A Thermo Fisher XL Orbitrap mass  
9 spectrometer, with electrospray ionization was employed with the needle potential held at 4.5  
10 kV. Tandem mass spectrometry conditions used were 2 mTorr helium collision gas and 25-35  
11 eV collision potential. Ions of interest were put on a data dependent mass list and if encountered  
12 were fragmented. Positive ion mode full scan (200–750 Da) was conducted with a scan time of  
13 0.73 s. Ultraviolet data collection was performed over a scan range of 200 to 400 nm with 2 Hz  
14 data collection frequency. Xcalibur software (version 2.0) was used to acquire all data.

15  
16  
17  
18  
19  
20  
21  
22  
23  
24  
25  
26  
27  
28  
29  
30  
31 **Metabolism of Bromfenac to Indolinone.** The time-dependent degradation of **1** (1 µM) in  
32 HLM (1 mg total protein/ml) with alamethicin (10 µg/ml) and MgCl<sub>2</sub> (5 mM) was performed to  
33 quantify metabolism of **1** and the formation of **2**. Incubations were conducted in Tris buffer.<sup>13</sup>  
34 Aliquots (50 µl) were taken from the incubation (300 µl total) at 0, 30, 60, 120 and 240 min in  
35 the presence and absence of UDPGA (1 mM). The aliquots at each time point were added to  
36 quench solution (100 µL) containing internal standard, carbamazepine (50 nM). Samples were  
37 centrifuged and the supernatant was diluted 1:1 v:v with HPLC grade water and then analyzed by  
38 LC-MS/MS. The concentration of **1** and the amounts of **2** formed were determined from  
39 standard curves of peak area ratios (peak area of analyte/peak area of IS).

40  
41  
42  
43  
44  
45  
46  
47  
48  
49  
50  
51 The LC-MS/MS conditions were as follows: Sciex API 4000 (Waltham, MA, USA) mass  
52 spectrometer was run in positive ion mode with the Turbo Spray source with the following  
53  
54  
55  
56  
57  
58  
59  
60

1  
2  
3 source conditions; Collision gas set to 6, Curtain gas set to 25, Ion source gas 1 and 2 set to 30,  
4  
5 IonSpray voltage set to 5000 and the temperature set to 600 °C with the interface heater on. The  
6  
7 declustering potential was set at 90 volts for all of the compounds and the dwell time for each ion  
8  
9 was set to 50 msec. The transition ions in the MRM method (Q1 → Q3) for **1** were  $m/z$  334  
10  
11 →288 with the collision energy set to 25 volts, the MRM method for **2** were  $m/z$  316→183 with  
12  
13 the collision energy set to 30 volts and CBZ were  $m/z$  237→194 with the collision energy set to  
14  
15 27 volts. The LC system included a CTC Pal autosampler and ThermoElectron (Waltham, MA)  
16  
17 Accela 1250 binary pump. The mobile phases were 0.1% aqueous formic acid (solvent A) and  
18  
19 acetonitrile with 0.1% formic acid (solvent B). The injection volume was 5  $\mu$ l and the flow rate  
20  
21 was 900  $\mu$ l/min with the step gradient starting at 95% A for 10 sec then stepping to 85% B  
22  
23 isocratic for 30 sec then stepping back to 95% A for another 30 sec. The column used was a  
24  
25 Phenomenex (Torrance, CA) Kinetex 5  $\mu$ m C18 100Å 30 x 2.1 mm.  
26  
27  
28  
29  
30  
31  
32  
33  
34  
35  
36  
37  
38  
39  
40  
41  
42  
43  
44  
45  
46  
47  
48  
49  
50  
51  
52  
53  
54  
55  
56  
57  
58  
59  
60

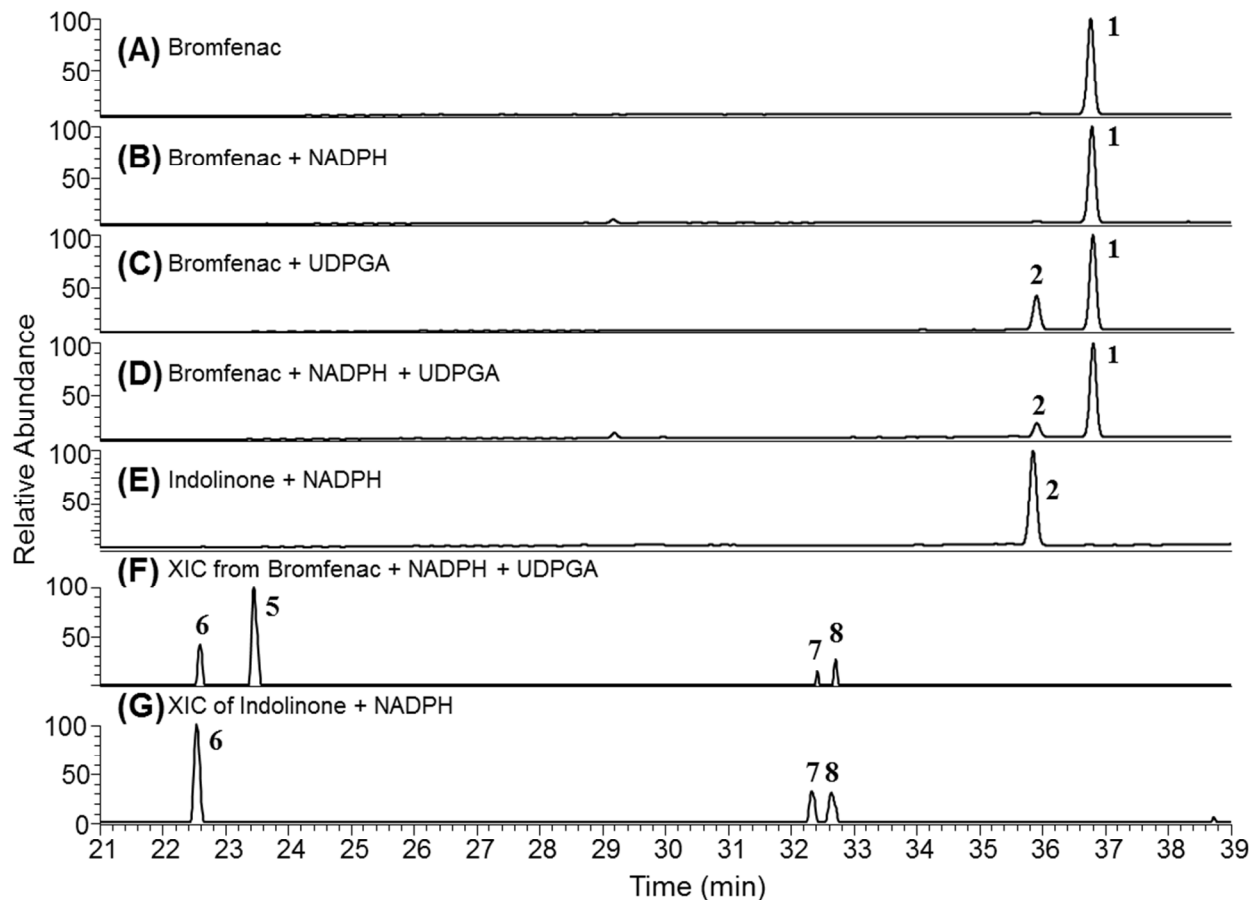


**Figure 2.** Chromatograms of 60 min incubations in HLM with **1** (rt = 36.8 min) with (A) no cofactors, (B) NADPH, (C) is with UDPGA and (D) UDPGA and NADPH. (E) **2** standard incubated with NADPH (rt = 35.9 min). (F) is the extracted ion chromatogram of exact  $m/z$  of 493.0063 (rt = 22.5, 32.2 and 32.6 min) and 511.0169 (rt = 23.4 min) of HLM incubations with **1** and UDPGA and NADPH and (G) is **2** with NADPH. All incubations include NAC at 5 mM.

## Results

**Metabolite Identification Experiments.** Qualitative high resolution LC-MS/MS analysis with ultraviolet (UV) detection of liver microsome incubations containing **1** with UDPGA and alamethicin led to an increase in the formation of a large UV peak at retention time (rt) 35.9 min

1  
2  
3 (Figure 2). The peak contained exact  $m/z$  of 315.9968 corresponding to a molecular formula of  
4  $C_{15}H_{11}BrNO_2^+$  within 5 ppm. The mass spectrum and retention time of the synthetic standard of  
5  
6 the **2** matched the peak of the metabolite formed from the **1** incubations at  $rt$  35.9 min (Figure  
7  
8 2C, 2D and 2E).  
9

10  
11  
12 Liver microsome incubations with NADPH, UDPGA, alamethicin and NAC with **1** and **2** led  
13  
14 to the detection of the three thiol conjugates with an  $m/z$  equal to 493.0063 and one with an  $m/z$   
15  
16 of 511.0169. The  $m/z$  of 493.0063 is consistent with that of **2** with one atom of oxygen and one  
17  
18 molecule of NAC added. This exact mass corresponds to the molecular formula  
19  
20  $C_{20}H_{18}BrN_2O_6S^+$ . The  $m/z$  of 511.0169 is consistent with that of **1** with one atom of oxygen and  
21  
22 one molecule of NAC added; corresponding to the molecular formula  $C_{20}H_{20}BrN_2O_7S^+$ .  
23  
24  
25

26  
27 The high resolution full scan of **1** at  $rt$  36.7 min corresponds to a  $m/z$  334.0073 which  
28  
29 corresponds to a molecular formula of  $C_{15}H_{13}BrNO_3^+$ . The product ion scan contains ions of  $m/z$   
30  
31 315.9968, 288.0019 and 182.9440. The ion at 315.9968 is the neutral loss of water from **1**, the  
32  
33 ion at 288.0019 is the loss of  $CO_2$  with charge retention on the carbocation. The ion at  $m/z$  of  
34  
35 182.9440 corresponds to the 4-bromobenzyloxonium ion. This ion is conserved in the product  
36  
37 ion scan of the **2** ( $rt$  = 35.8 min). These spectrum are found in the supporting data in Figure S1  
38  
39 and S2.  
40  
41

42  
43 The NAC adduct at retention time 22.5 min (**6**) had the CID spectrum shown in Figure 3A and  
44  
45 had ions at  $m/z$  180.0114, 182.9440, 206.0270 and 293.0591. The fragment ion with  $m/z$  of  
46  
47 182.9440 corresponds to a 4-bromobenzyloxonium ion. The fragment ion at  $m/z$  180.0114 was  
48  
49 assigned as the product of a neutral loss of 4-bromobenzylaldehyde and cleavage adjacent to the  
50  
51 cysteinyl thioether moiety, with charge retention on the indolinone moiety containing oxygen  
52  
53 and sulfur atoms attached; this corresponds to a molecular formula of  $C_8H_6NO_2S^+$ . The presence  
54  
55  
56  
57  
58  
59  
60

1  
2  
3 of these two fragment ions is consistent with an aromatic thioether motif on the  
4 hydroxyindolinone moiety.  
5  
6

7  
8 The NAC adduct which corresponds to the hydroxylated bromfenac (**5**),  $m/z$  of 511.0169, had  
9 the product ion spectra shown in Figure 3B and retention time of 23.4 min. The spectrum  
10 contains the presence of the 4-bromobenzyloxonium ion with  $m/z$  182.9440. The presence of this  
11 ion indicates hydroxylation and NAC have been added to the 2-aminophenylacetic acid moiety  
12 of the metabolite. The ion at  $m/z$  293.0591 (Figure 3B) also contributes to the evidence of the  
13 NAC and oxygen adding to the 2-aminophenylacetic acid.  
14  
15  
16  
17  
18  
19  
20

21  
22 The NAC adducts at retention time 32.2 min (**7**) and 32.6 min (**8**) had very similar product ion  
23 spectra shown in Figure 3C and 3D. The NAC adducts contained the ions at  $m/z$  182.9440 and  
24 329.9760. The fragment ion with  $m/z$  of 182.9440 corresponds with a 4-bromobenzyloxonium  
25 ion. The fragment ion at  $m/z$  329.9760 was assigned as the homolytic cleavage product with a  
26 neutral loss of the NAC; the charge is retained on the hydroxylated indolinone moiety  
27 corresponding to a molecular formula of  $C_{15}H_9BrNO_3^+$ . The presence of these two fragment ions  
28 is consistent with an aliphatic thioether motif on the hydroxyindolinone moiety.<sup>14</sup>  
29  
30  
31  
32  
33  
34  
35  
36

37  
38 Rat and cynomologus monkey liver microsomes were incubated with **1** in the presence of  
39 UDPGA, NADPH, NAC and alamethicin. The extracted ion chromatograms are found in Figure  
40 4 with a comparison to HLM. Compared to HLM, **5** and **6** were formed in lesser proportion to **7**  
41 and **8** in RLM. Comparing CLM to HLM, **6** seemed to be formed in a greater proportion to **7** and  
42 **8** and **5** was not detected (Figure 4). All three of the **2** NAC adducts, **6**, **7** and **8**, were detected in  
43 RLM and CLM. The retention times and spectra of the product ion scans of the NAC adducts  
44 were consistent with those found in HLM.  
45  
46  
47  
48  
49  
50  
51  
52  
53  
54  
55  
56  
57  
58  
59  
60

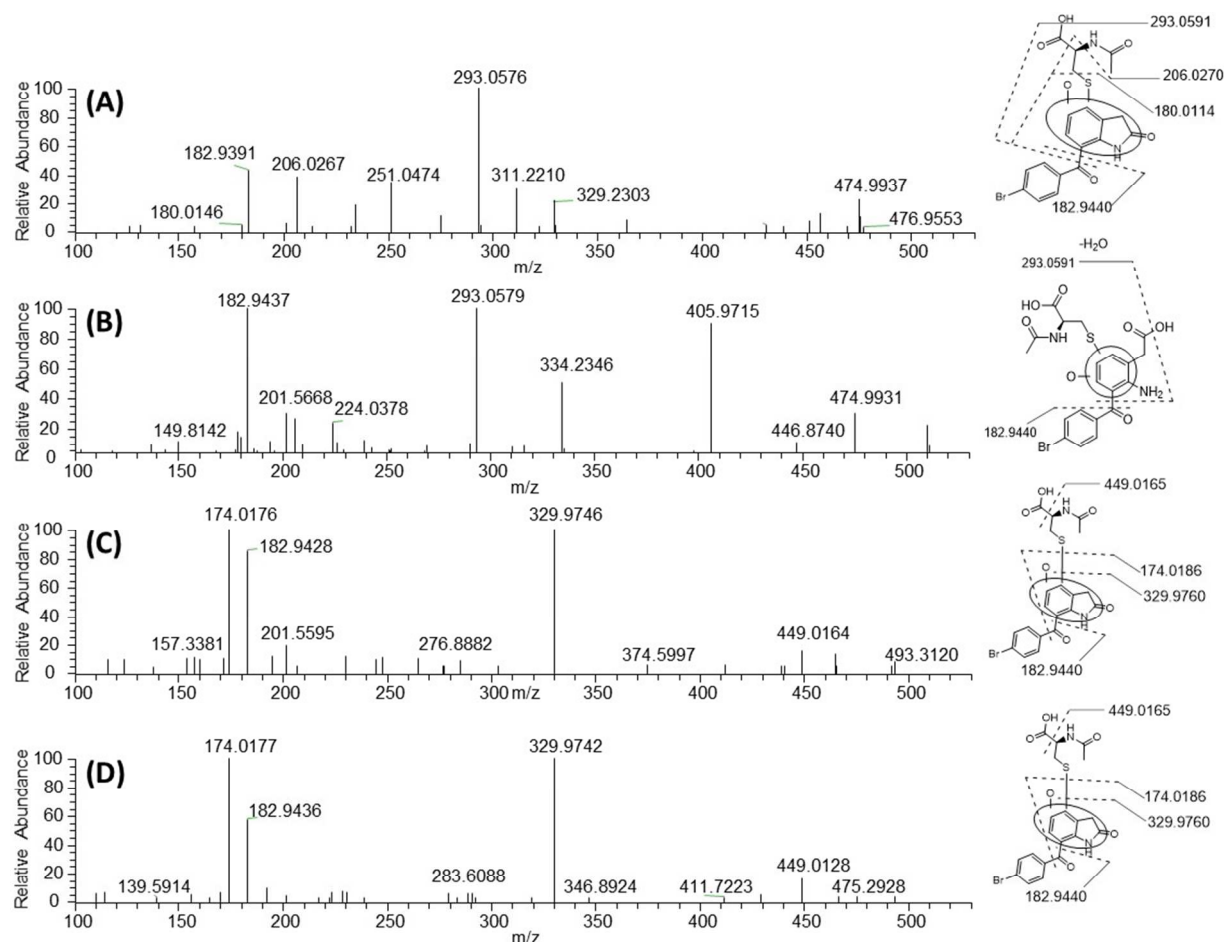


**Figure 3.** Product ion spectrum of (A) **6** with  $m/z$  493.0063 at retention time 22.5 min (B) **5** with  $m/z$  of 511.0169 at retention time of 23.4 min (C) **7** with  $m/z$  493.0063 at retention time 32.3 min (D) **8** with  $m/z$  493.0063 at retention time 32.6 min. Incubations were conducted in HLM with 20  $\mu\text{M}$  **1** for 60 minutes with UDPGA, NADPH, NAC and alamethicin.

**1** was incubated with human hepatocytes to determine if reactive intermediates can form in a whole cell system and be trapped by the endogenous nucleophile; glutathione (GSH). HLM with NADPH, UDPGA, alamethicin and GSH were also incubated as a control experiment. The results indicated that similar reactive intermediates are trapped with HLM with NAC. In the HLM experiments, four GSH adducts were found. One adduct (rt 18.94 min) is consistent with **3** and the addition of GSH to the 2-aminophenylacetic acid moiety matching  $m/z$  of 655.0704. The

1  
2  
3 product ion spectrum of the adduct contains the ions with  $m/z$  of 182.9440 and 379.9587, which  
4  
5 adds to the evidence. The other three adducts (rt 18.3, 25.2, and 25.4 min) are consistent with **4**  
6  
7 with GSH added. The  $m/z$  is equal to 637.0598, and is similar to the adducts described above  
8  
9 with NAC as the trapping agent. All three product ion spectra include  $m/z$  of 182.9440 which  
10  
11 corresponds to the 4-bromobenzyloxonium ion. Interestingly, in the hepatocyte incubations only  
12  
13 three GSH adducts were found, two from **4** and one from **3**. One of the adducts, which we  
14  
15 speculate to be formed from a quinone methide intermediate of **4**, was not present in the human  
16  
17 hepatocyte experiment (Figure S4).  
18  
19  
20  
21  
22  
23

#### 24 **Bromfenac Stability and Formation of Indolinone Metabolite.**

25  
26 **1** was incubated in HLM with UDPGA containing alamethicin and the loss of **1** and formation  
27  
28 of **2** was quantified using the synthetic standard. The incubation was monitored over the course  
29  
30 of 240 min and approximately 0.5  $\mu\text{M}$  of **1** was metabolized to 0.5  $\mu\text{M}$  of **2** (Figure 5).  
31  
32  
33  
34  
35  
36  
37  
38  
39  
40  
41  
42  
43  
44  
45  
46  
47  
48  
49  
50  
51  
52  
53  
54  
55  
56  
57  
58  
59  
60

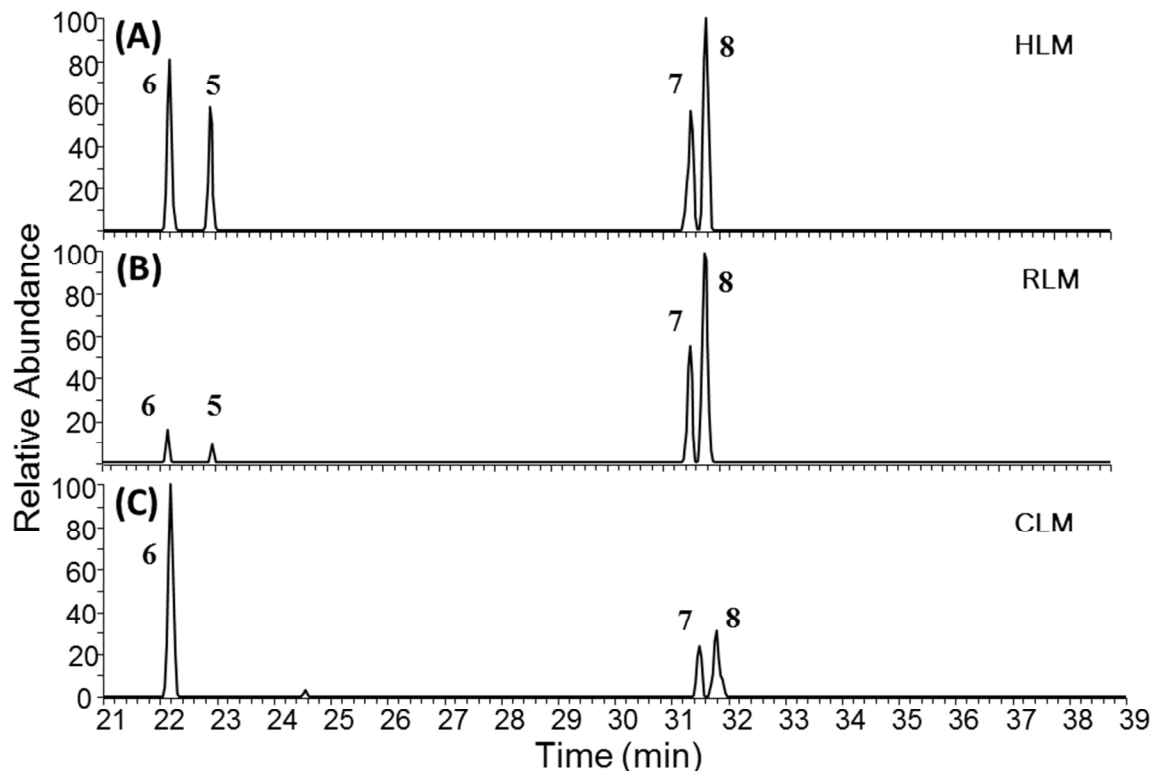


**Figure 4.** Chromatograms of 60 min incubations of **1** with NAC, UDPGA, alamethicin and NADPH in (A) human liver microsomes (B) rat liver microsomes, and (C) cynomolgus monkey liver microsomes. Extracted ion chromatogram of **4**+ NAC with exact mass  $m/z$  493.0063 (**6**, **7**, and **8**) and **5** with exact mass  $m/z$  511.0169.

## Discussion

**1** bioactivation has been studied since the compound was withdrawn from the market in 1998 and has since been reviewed in the literature.<sup>6,15</sup> Working from the hypothesis that DILI can arise from the formation of reactive metabolites and covalent binding to cellular macromolecules, a few studies have been done to elucidate the mechanism of covalent binding of bromfenac.<sup>6</sup> Following up on Usiu *et al* 2009, we attempt to address the NADPH and UDPGA dependence of bromfenac covalent binding to HLMs.

1  
2  
3 We propose that an UDPGA-dependent acyl glucuronide intermediate forms. Acyl-  
4 glucuronides and esters in general are susceptible to hydrolysis by free amines.<sup>16</sup> This unstable  
5 intermediate undergoes intramolecular nucleophilic substitution via addition-elimination to form  
6 the bromfenac indolinone metabolite (Scheme 1). In this reaction, we propose the free amine  
7 functions as the nucleophile, attacking the electrophilic carbonyl carbon of the acyl glucuronide  
8 ester to form a tetrahedral intermediate. The tetrahedral intermediate collapses, eliminating the  
9 glucuronic acid and reforming the carbonyl to provide the **2**. This mechanism is also supported  
10 by the acid catalyzed synthesis of **2**. When the carboxylic acid is protonated with the addition of  
11 acid, the alcohol makes for a better leaving group, thereby facilitating the formation of the  
12 indolinone.<sup>17</sup>

13  
14  
15 For additional confirmation of this finding, **1** was incubated in HLM with UDPGA, and the  
16 loss of **1** and formation of the **2** was quantified. Over a 240 min incubation, approximately 0.5  
17  $\mu\text{M}$  of **1** was metabolized to 0.5  $\mu\text{M}$  of **2** (Figure 5). This result demonstrates the UDPGA- and  
18 time dependent- formation of **2** from **1**, since formation of **2** was not detected in HLM in the  
19 absence of UDPGA.

20  
21  
22 It is unlikely the acyl glucuronide intermediate could be the cause of covalent binding to  
23 proteins due to the equal loss of **1** and formation of **2**; this leaves little room for binding to other  
24 reactants. Literature evidence exists for intramolecular reactions occurring at very favorable  
25 rates due to the effective high concentrations of reactants. Furthermore, intramolecular reactions  
26 are entropically favored as opposed to intermolecular reactions which require bringing two  
27 separate molecules together.<sup>18,19</sup> It should be noted that in Usui *et al*'s work, there was a small  
28 amount of covalent binding to the HLM proteins with NADPH alone which could be attributed  
29 to the reactive intermediate that leads to **5** with retention time of 23.4 min (Figure 2F and 3B).

1  
2  
3 The metabolism of the **2** was investigated since it originates from a glucuronidation pathway  
4 and is the largest metabolite found in human urine.<sup>4</sup> To see if the synthetically prepared standard  
5 could undergo further P450 metabolism to a chemically-reactive intermediate, **2** was incubated  
6 in liver microsomes. Three NAC adducts were found when **2** was incubated in HLM with NAC  
7 and NADPH (Scheme 1 and Figure 2G). Each NAC adduct was confirmed to have the isotopic  
8 distribution pattern of bromine with an  $m/z$  peak 1.9979 Dalton higher at approximately 98% of  
9 the original  $m/z$  peak of interest in the full scan mass spectrum. No other major metabolites were  
10 detected by UV traces in liver microsome incubations with **2** and the NAC adducts could only be  
11 found by extracting the ions of interest (Figure 2F, 2G).

12  
13  
14 In order to ensure these NAC adducts were formed from **1** as the starting material, **1** was  
15 incubated in LM with NADPH, UDPGA, NAC and alamethicin. The results indicate an increase  
16 in the formation of **2** at rt 36.0 min (Figure 2D and 2E). There were also four NAC adducts  
17 found by LC-MS/MS (Figure 2), three of which have consistent retention time and product ion  
18 spectra with the NAC adducts detected in the incubation with **2** (Figure 3).

19  
20  
21 One proposed mechanism leading to **6** could be oxidation of the indolinone moiety *para* to the  
22 amine, which can undergo a further two electron oxidation to an electrophilic quinone-imine  
23 intermediate (Scheme 1). This intermediate can undergo adduction by NAC at the two open  
24 aromatic carbons *meta* to the amine. While there is a possibility for thioether formation at each  
25 of the two open *meta* positions, only one adduct was found. One explanation for this could be  
26 the steric hindrance of one position over the other. Another possible mechanism is that the  
27 hydroxylation and thioether formation could go through an epoxidation mechanism, although  
28 this would be better supported with two peaks in the chromatogram. The structure is supported  
29 by another fragment which has an  $m/z$  180.0114 in the fragmentation of **6** (Figure 2F). This  
30  
31  
32  
33  
34  
35  
36  
37  
38  
39  
40  
41  
42  
43  
44  
45  
46  
47  
48  
49  
50  
51  
52  
53  
54  
55  
56  
57  
58  
59  
60

1  
2  
3 corresponds to the indolinone moiety with sulfur and oxygen attached, which we speculate is the  
4 NAC and oxygen attached to the aromatic ring. There are literature examples that show when  
5 quinone-imines are formed, the nucleophilic thiols can attach to the aromatic ring at the *ortho* or  
6 *meta* position to the hydroxyl group.<sup>20,21</sup> Thioether adducts that retain the sulfur atom upon  
7 fragmentation are characteristically found to be attached to carbons in aromatic rings.<sup>14</sup>

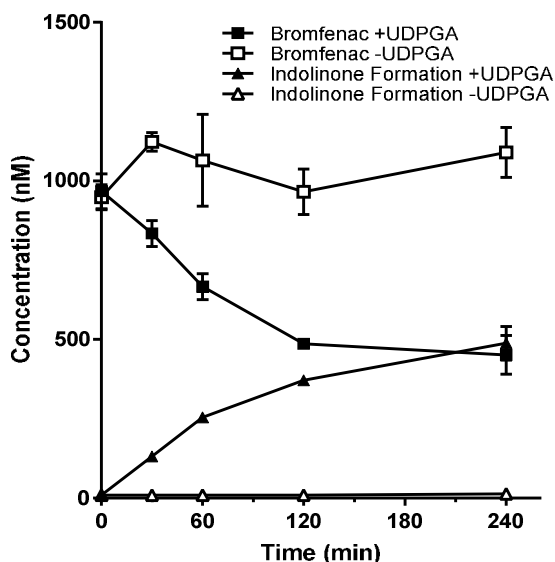
8  
9  
10 We hypothesize that the thioether adducts at retention times 32.2 min (7) and 32.6 min (8)  
11 formed from **2** are due to hydroxylation *ortho* and *para* to the methylene carbon. After a further  
12 two electron oxidation, the resulting intermediates are quinone methides (Scheme 1). In this  
13 intermediate, the methide carbon would be the most electron deficient and susceptible to  
14 nucleophilic addition of nucleophilic thiols.<sup>22</sup> This is supported by the homolytic cleavage of the  
15 sulfur and the hydroxylated indolinone ions in the product ion spectra of the peaks (Figure 3C  
16 and 3D). Another possible explanation for the aromatic thioether adducts could be addition of  
17 NAC on the aromatic ring from the quinone methide reactive intermediates, where there are  
18 potentially reactive  $\alpha,\beta$  unsaturated ketones. However, thiols reacting with the aromatic ring in  
19 quinone methides is not supported by the literature.<sup>23,24,25</sup>

20  
21  
22 If the NAC adducts result from the formation of quinone methide intermediates and attach to  
23 the aliphatic carbon of the indolinone moiety, there is a possibility of forming two diastereomers  
24 on the prochiral benzylic position as opposed to the oxidative isomers we propose in Scheme 1.<sup>26</sup>  
25 With two chiral centers present it is possible to separate them on a reverse phase C18 column.  
26 To test which hypothesis is correct, we incubated **2** with HLM and  $\beta$ -mercaptoethanol, a thiol  
27 with no chiral center. After extraction of the exact mass  $m/z$  407.9900 from the LC-MS trace,  
28 three peaks were found. The exact mass corresponds to **4** with the addition of  $\beta$ -mercaptoethanol,  
29  
30  
31  
32  
33  
34  
35  
36  
37  
38  
39  
40  
41  
42  
43  
44  
45  
46  
47  
48  
49  
50  
51  
52  
53  
54  
55  
56  
57  
58  
59  
60

1  
2  
3 matching the molecular formula of  $C_{17}H_{15}BrNO_4S^+$ . Finding three adduct peaks in this  
4  
5 experiment supports the hypothesis of oxidative isomers and not diastereomers (Figure S3).  
6  
7

8 Similar structures of thioether adducts were found when bromfenac was incubated in HLM and  
9  
10 human hepatocytes fortified with GSH (Figure S4). One of the proposed quinone methide  
11  
12 metabolites was not found. A major difference between GSH and NAC is the size of the  
13  
14 molecule; we speculate that since NAC is smaller it can potentially fit into active sites more  
15  
16 easily than GSH. Thus, GSH may not fit in the active site of the P450 where the reactive  
17  
18 intermediate is formed.  
19  
20

21 Complete structural analysis of the adducts could be difficult to fully assign unless synthetic  
22  
23 standards are made or enough material can be collected from liver microsome incubations and  
24  
25 analyzed by two dimensional NMR. Collecting sufficient sample from microsome incubations  
26  
27 has been challenging and is the focus of ongoing efforts of our lab.  
28  
29  
30  
31  
32  
33



34  
35  
36  
37  
38  
39  
40  
41  
42  
43  
44  
45  
46  
47  
48  
49  
50  
51  
52  
53 **Figure 5.** Disappearance of **1** with and without UDPGA and the formation of the **2** with and  
54  
55 without UDPGA in incubations in human liver microsomes.  
56  
57  
58  
59  
60

1  
2  
3 Since these thiol adducts could only be detected by extracting their exact masses, it brings into  
4 question their relevance to **1** bioactivation. One possible explanation for the lack of sensitivity is  
5 that these reactive intermediates are covalently bound to microsomal proteins, since the covalent  
6 binding of **1** has been previously demonstrated.<sup>6</sup> Another possible explanation for the relevance  
7 of these reactive intermediates is that **1** was approved for only a ten day duration of use, and  
8 there may be some buildup of reactive intermediates. Potential evidence is found in a preclinical  
9 toxicology study where glutathione depletion in rat liver was observed.<sup>5</sup>

10  
11 In summary, we have found evidence for the formation of reactive metabolites of **1**. One  
12 pathway for the bioactivation requires oxidation of **1** followed by thioether adduct formation.  
13 Another pathway of bioactivation requires a short-lived acyl glucuronide intermediate which  
14 results in the formation of **2**. **2** requires further oxidation by P450 on every open carbon on the  
15 aromatic ring of the indolinone moiety. These hydroxylated metabolites require a further  
16 oxidation to form the quinone-imine and quinone methide intermediates. This bioactivation  
17 pathway contributes to the body of evidence which may help to understand the mechanisms of  
18 toxicity resulting from **1** use in the clinic. Reactive metabolites are not the only cause of  
19 hepatotoxicity and/or cholestasis; other potential sources include the inhibition of transporters  
20 including bile salt excretory pump.<sup>27</sup>

### 21 22 23 24 25 26 27 28 29 30 31 32 33 34 35 36 37 38 39 40 41 42 43 44 **Supporting Information.**

45 MS/MS interpreted spectrum of bromfenac and bromfenac indolinone. Chromatograms of XIC  
46 of glutathione adducts and  $\beta$ -mercaptoethanol adducts. Interpreted spectrum of GSH adducts  
47 (PDF).

### 48 49 50 51 52 53 54 **Corresponding Author**

1  
2  
3 \* Tel: 650-741-0928. E-mail: jdriscoll@myokardia.com  
4  
5

### 6 **Present Addresses**

7  
8  
9 333 Allerton Ave. South San Francisco CA 94080  
10  
11

### 12 **Author Contributions**

13  
14 The manuscript was written by James P. Driscoll and Aprajita S. Yadav. Experiments were  
15 performed by all of the authors. All authors have given approval to the final version of the  
16 manuscript.  
17  
18  
19  
20  
21

### 22 **Funding Sources**

23  
24 All funds used to support the research of the manuscript were provided by MyoKardia, Inc.,  
25  
26  
27

### 28 **ACKNOWLEDGMENT**

29  
30  
31 The authors would like to thank Drs. Mark P. Grillo and Tim Carlson for useful discussion and  
32 review of the manuscript. We would like to thank Jasleen K. Sodhi for helpful review of the  
33 manuscript. We would like to thank Drs. Danielle Aubele and Brian Kane for purification and <sup>1</sup>H  
34 NMR of bromfenac indolinone.  
35  
36  
37  
38  
39  
40

### 41 **ABBREVIATIONS**

42  
43 NSAID, nonsteroidal anti-inflammatory drug; NADPH, nicotinamide adenosine diphosphate  
44 reduced; UDPGA, uridine diphosphate glucuronic acid; HLM, human liver microsomes; LC-  
45 MS-UV, liquid chromatography mass spectrometry ultraviolet detection; NMR, nuclear  
46 magnetic resonance; ml, milliliter; mg milligram, NAC, N-acetylcysteine; AST ALT  
47  
48  
49  
50  
51

### 52 **REFERENCES**

53  
54  
55 (1) Rabkin, J. M., Smith, M. J., Orloff, S. L., Corless, C. L., Stenzel, P., and Olyaei, A. J. (1999)  
56  
57  
58  
59  
60

1  
2  
3 Fatal fulminant hepatitis associated with bromfenac use. *Ann. Pharmacother.* 33, 945–947.  
4

5  
6 (2) Moses, P. L., Schroeder, B., Alkhatib, O., Ferrentino, N., Suppan, T., and Lidofsky, S. D.  
7  
8 (1999) Severe hepatotoxicity associated with bromfenac sodium. *Am. J. Gastroenterol.* 94,  
9  
10 1393–1396.  
11

12  
13  
14 (3) Fontana, R. J., McCashland, T. M., Benner, K. G., Appelman, H. D., Gunartanam, N. T.,  
15  
16 Wisecarver, J. L., Rabkin, J. M., and Lee, W. M. (1999) Acute liver failure associated with  
17  
18 prolonged use of bromfenac leading to liver transplantation. *Liver Transplant. Surg.* 5, 480–484.  
19  
20

21  
22 (4) Osman, M., Chandrasekaran, A., Chan, K., Scatina, J., Ermer, J., Cevallos, W., and  
23  
24 Sisenwine, S. F. (1998) Metabolic disposition of <sup>14</sup>C-bromfenac in healthy male volunteers. *J.*  
25  
26 *Clin. Pharmacol.* 38, 744-752  
27

28  
29  
30 (5) Peters, T. S. (2005) Do Preclinical Testing Strategies Help Predict Human Hepatotoxic  
31  
32 Potentials? *Toxicol. Pathol.* 33, 146–154.  
33

34  
35  
36 (6) Usui, T., Mise, M., Hashizume, T., Yabuki, M., and Komuro, S. (2009) Evaluation of the  
37  
38 Potential for Drug-Induced Liver Injury Based on in Vitro Covalent Binding to Human Liver  
39  
40 Proteins. *Drug Metab. Dispos.* 37, 2383–2392.  
41

42  
43  
44 (7) Kirkman, S. K., Zhang, M. Y., Horwatt, P. M., and Scatina, J. (1998) Isolation and  
45  
46 identification of bromfenac glucoside from rat bile. *Drug Metab. Dispos.* 26, 720–3.  
47

48  
49  
50 (8) Stepan, A. F., Walker, D. P., Bauman, J., Price, D. a, Baillie, T. a, Kalgutkar, A. S., and Aleo,  
51  
52 M. D. (2011) Structural alert/reactive metabolite concept as applied in medicinal chemistry to  
53  
54 mitigate the risk of idiosyncratic drug toxicity: a perspective based on the critical examination of  
55  
56  
57  
58  
59  
60

1  
2  
3 trends in the top 200 drugs marketed in the United States. *Chem. Res. Toxicol.* 24, 1345–410.  
4  
5

6 (9) Williams, D. P., and Park, B. K. (2003) Idiosyncratic toxicity: The role of toxicophores and  
7 bioactivation. *Drug Discov. Today* 8, 1044–1050.  
8  
9

10 (10) Grillo, M. P., and Lohr, M. T. (2009) Covalent binding of phenylacetic acid to protein in  
11 incubations with freshly isolated rat hepatocytes. *Drug Metab. Dispos.* 37, 1073–82.  
12  
13  
14

15 (11) Bambal, R. B., and Hanzlik, R. P. (1995) Bromobenzene 3,4-oxide alkylates histidine and  
16 lysine side chains of rat liver proteins in vivo. *Chem. Res. Toxicol.* 8, 729–35.  
17  
18  
19

20 (12) Sodhi, J. K., Delarosa, E. M., Halladay, J. S., Driscoll, J. P., Mulder, T., Dansette, P. M.,  
21 and Khojasteh, S. C. (2017) Inhibitory Effects of Trapping Agents of Sulfur Drug Reactive  
22 Intermediates against Major Human Cytochrome P450 Isoforms. *Int. J. Mol. Sci.* 18, 1553.  
23  
24  
25  
26  
27

28 (13) Walsky, R. L., Bauman, J. N., Bourcier, K., Giddens, G., Lapham, K., Negahban, A., Ryder,  
29 T. F., Obach, R. S., Hyland, R., and Goosen, T. C. (2012) Optimized assays for human UDP-  
30 glucuronosyltransferase (UGT) activities: Altered alamethicin concentration and utility to screen  
31 for UGT inhibitors. *Drug Metab. Dispos.* 40, 1051–1065.  
32  
33  
34  
35  
36  
37  
38

39 (14) Xie, C., Zhong, D., and Chen, X. (2013) A fragmentation-based method for the  
40 differentiation of glutathione conjugates by high-resolution mass spectrometry with electrospray  
41 ionization. *Anal. Chim. Acta* 788, 89–98.  
42  
43  
44  
45  
46  
47  
48

49 (15) Park, B. K., Boobis, A., Clarke, S., Goldring, C. E. P., Jones, D., Kenna, J. G., Lambert, C.,  
50 Laverty, H. G., Naisbitt, D. J., Nelson, S., Nicoll-Griffith, D. a, Obach, R. S., Routledge, P.,  
51 Smith, D. a, Tweedie, D. J., Vermeulen, N., Williams, D. P., Wilson, I. D., and Baillie, T. a.  
52  
53  
54  
55  
56  
57  
58  
59  
60

1  
2  
3 (2011) Managing the challenge of chemically reactive metabolites in drug development. *Nat.*  
4  
5 *Rev. Drug Discov.* 10, 292–306.  
6

7  
8 (16) Vaz, A. D. N., Wang, W. W., Bessire, A. J., Sharma, R., and Hagen, A. E. (2010) A rapid  
9 and specific derivatization procedure to identify acyl-glucuronides by mass spectrometry. *Rapid*  
10 *Commun. Mass Spectrom.* 24, 2109–2121.  
11  
12  
13

14  
15 (17) Testa, B., and Krämer, S. D. (2007) The biochemistry of drug metabolism--an introduction:  
16 part 3. Reactions of hydrolysis and their enzymes. *Chem. Biodivers.* 4, 2031–122.  
17  
18  
19

20 (18) Capon, B. (1964) Neighbouring group participation. *Q. Rev. Chem. Soc.* 18, 45.  
21  
22  
23

24 (19) Menger, F. M. (1985) On the source of intramolecular and enzymatic reactivity. *Acc. Chem.*  
25 *Res.* 18, 128–134.  
26  
27  
28

29 (20) Zheng, J., Ma, L., Xin, B., Olah, T., Humphreys, W. G., and Zhu, M. (2007) Screening and  
30 identification of GSH-trapped reactive metabolites using hybrid triple quadrupole linear ion trap  
31 mass spectrometry. *Chem Res Toxicol* 20, 757–766.  
32  
33  
34  
35

36 (21) Chen, W., Shockcor, J. P., Tonge, R., Hunter, A., Gartner, C., and Nelson, S. D. (1999)  
37 Protein and nonprotein cysteinyl thiol modification by N-acetyl-p- benzoquinone imine via a  
38 novel Ipso adduct. *Biochemistry* 38, 8159–8166.  
39  
40  
41  
42  
43  
44

45 (22) Thompson, D. C., Thompson, J. A., Sugumaran, M., and Moldéus, P. (1993) Biological and  
46 toxicological consequences of quinone methide formation. *Chem. Biol. Interact.* 86, 129–162.  
47  
48  
49

50 (23) Driscoll, J. P., Kornecki, K., Wolkowski, J. P., Chupak, L., Kalgutkar, A. S., and  
51 O'Donnell, J. P. (2007) Bioactivation of phencyclidine in rat and human liver microsomes and  
52  
53  
54  
55  
56  
57  
58  
59  
60

1  
2  
3 recombinant P450 2B enzymes: evidence for the formation of a novel quinone methide  
4 intermediate. *Chem. Res. Toxicol.* 20, 1488–97.  
5  
6

7  
8  
9 (24) Thompson, J. A., Carlson, T. J., Sun, Y., Dwyer-Nield, L. D., and Malkinson, A. M. (2001)  
10 Studies using structural analogs and inbred strain differences to support a role for quinone  
11 methide metabolites of butylated hydroxytoluene (BHT) in mouse lung tumor promotion.  
12  
13 *Toxicology* 160, 197–205.  
14  
15

16  
17  
18 (25) Toteva, M. M., and Richard, J. P. (2011) The generation and reactions of quinone methides.  
19  
20 *Adv. Phys. Org. Chem.* Elsevier Inc. 45, 39-91  
21  
22

23  
24 (26) Thompson, D. C., Perera, K., Krol, E. S., and Bolton, J. L. (1995) O-Methoxy-4-  
25  
26 alkylphenols That Form Quinone Methides of Intermediate Reactivity Are the Most Toxic in Rat  
27  
28 Liver Slices. *Chem. Res. Toxicol.* 8, 323–327.  
29  
30

31  
32 (27) Woodhead, J. L., Yan, K., Siler, S. Q., Watkins, P. B., Brouwer, K. L. R., Barton, H. A., and  
33  
34 Howell, B. A. (2014) Exploring BSEP inhibition-mediated toxicity with a mechanistic model of  
35  
36 drug-induced liver injury. *Front. Pharmacol.* 5, 1-11  
37  
38  
39  
40  
41  
42  
43  
44  
45  
46  
47  
48  
49  
50  
51  
52  
53  
54  
55  
56  
57  
58  
59  
60